Magnetic and electronic properties of Li_xCoO_2 single crystals

K. Miyoshi,[1] C. Iwai,[1] H. Kondo,[1] M. Miura,[1] S. Nishigori,[2] and J. Takeuchi[1]
[1]*Department of Material Science, Shimane University, Matsue 690-8504, Japan*
[2]*Department of Materials Analysis, CIRS, Shimane University, Matsue 690-8504, Japan*
(Received 22 May 2010; revised manuscript received 14 July 2010; published 10 August 2010)

Measurements of electrical resistivity (ρ), dc magnetization (M), and specific heat (C) have been performed on layered oxide Li_xCoO_2 ($0.25 \leq x \leq 0.99$) using single-crystal specimens. The ρ versus temperature (T) curve for $x=0.90$ and 0.99 is found to be insulating but a metallic behavior is observed for $0.25 \leq x \leq 0.71$. At $T_S \sim 155$ K, a sharp anomaly is observed in the ρ-T, M-T, and C/T-T curves for $x=0.66$ with thermal hysteresis, indicating the first-order character of the transition. The transition at $T_S \sim 155$ K is observed for the wide range of $x=0.46-0.71$. It is found that the M-T curve measured after rapid cool becomes different from that after slow cool below T_F, which is ~ 130 K for $x=0.46-0.71$. T_F is found to agree with the temperature at which the motional narrowing in the ^{7}Li NMR linewidth is observed, indicating that the Li ions stop diffusing and order at the regular site below T_F. The ordering of Li ions below $T_F \sim 130$ K is likely to be triggered and stabilized by the charge ordering in CoO_2 layers below T_S.

DOI: 10.1103/PhysRevB.82.075113 PACS number(s): 75.40.Cx, 71.27.+a, 75.30.Kz

I. INTRODUCTION

Layered oxide Li_xCoO_2 has been intensively studied for the practical use as a high-energy-density cathode material in commercial Li ion batteries. Li_xCoO_2 consists of CoO_2 layers and interlayers of Li atoms alternatively stacked along c axis. The related material Na_xCoO_2, which is originally known as a large thermoelectric material,[1] has been a subject of intensive study since the discovery of superconductivity in $Na_xCoO_2 \cdot 1.3H_2O$ below $T_c \sim 5$ K.[2] In CoO_2 layers, Co ions are in a mixed-valence state nominally having spins of $S=0$ (Co^{3+}) and $S=1/2$ (Co^{4+}), and form a two-dimensional (2D) regular triangular lattice, where novel types of electronic behavior are expected due to the geometrical frustration. Indeed, Na_xCoO_2 exhibits a rich variety of intriguing electronic properties as Na content x increases, that is, superconductivity in the hydrated compound ($x \sim 0.35$),[2] an insulating ground state induced by charge ordering ($x=0.5$),[3–6] unusual large thermoelectric power with metallic conductivity ($x \sim 0.7$),[1] a mass-enhanced Fermi-liquid ground state analogous to LiV_2O_4 ($x \sim 0.75$),[7] and a spin-density-wave state ($x \geq 0.75$).[8]

Li_xCoO_2 has a similar structure with different stacking sequence of oxygen atom layers, where Li ions occupy the octahedral sites with three CoO_2 sheets per unit cell, while Na ions in Na_xCoO_2 occupy the prismatic sites with two CoO_2 sheets per unit cell. Li deintercalation from $LiCoO_2$ generates Co^{4+} (t_{2g}^5) ions in the 2D triangular lattice of Co^{3+} (t_{2g}^6) and leads to a hole doping in the t_{2g} orbitals. Although $LiCoO_2$ is known to be insulating, a metallic behavior is therefore expected for the delithiated compound Li_xCoO_2. It has been reported that electrical resistivity near room temperature decreases abruptly with decreasing x from 1 to ~ 0.9,[9,10] indicating a transition from insulator to metal. For Li_xCoO_2, a sharp decrease in dc magnetization[10–15] and increase in resistivity[7] have been observed below 160–170 K with wide range of Li content. This transition is of first order[14,15] and the occurrence of charge ordering in CoO_2 layers has been suggested.[12,15] The fully delithiated compound CoO_2 ($x=0$), which is also the end member of Na_xCoO_2, has been found to be a Pauli paramagnetic metal without electron correlation due to the lack of two dimensionality in the structure contrasting to A_xCoO_2 ($A=$Li, Na).[16] Some attempts to establish the electronic phase diagram of Li_xCoO_2 have been made through the synthesis for the full or nearly full range of x using an electrochemical reaction technique.[12,15] It is suggested that the critical Li content x_c at which the magnetic property changes from Pauli paramagnetic type to Curie-Weiss one is 0.35–0.45,[15] whereas x_c for Na_xCoO_2 is known to be 0.5.[3]

In Li_xCoO_2, various unconventional nature may be discovered as in Na_xCoO_2 due to the characteristic triangular CoO_2 layers included in common in A_xCoO_2. Thus, it is interesting to explore the electronic behaviors of Li_xCoO_2, and it also allows to throw further light on the origin of the intriguing properties of Na_xCoO_2. Despite the recent intensive studies, details of the intrinsic properties of Li_xCoO_2 still remain unclear. The investigations on Li_xCoO_2 have been so far limited to the powder samples. For the further understanding, detailed investigations on the microscopic nature using single-crystal specimens are highly desirable in the future study. For the purpose, it is an important first step to synthesize single-crystal specimens of Li_xCoO_2 with systematic change in x and survey the physical properties. In the present work, we have successfully synthesized single crystals of Li_xCoO_2 with $x=0.25-0.99$ and performed the measurements of dc magnetization, electrical resistivity, and specific heat. A first-order transition has been observed at $T_S \sim 155$ K for the specimen with $x=0.46-0.71$. We demonstrate that the transition at T_S is always followed by the ordering of Li ions below $T_F \sim 130$ K. This suggests the possibility that the ordering of Li ions is triggered and stabilized by the charge ordering in CoO_2 layers below T_S via Coulomb coupling.

II. EXPERIMENT

Single-crystal specimens of Li_xCoO_2 were prepared by chemically extracting lithium from $LiCoO_2$ single crystals

reacting with an oxidizer NO_2BF_4 in an acetonitrile medium. In the previous work, single crystals of $LiCoO_2$ were grown in an optical floating-zone furnace,[14] whereas in the present work those were obtained by an ion exchange reaction between Li_2CO_3 and $Na_{0.75}CoO_2$ single crystals, which are easier to obtain than $LiCoO_2$ single crystals. The single-crystal growth of $Na_{0.75}CoO_2$ was performed in a similar manner as described in the literature.[17] Single crystals of $Na_{0.75}CoO_2$ cleaved to a thickness of ~0.2 mm were embedded in Li_2CO_3 powder in an alumina boat and heated in air at 600 °C for 24 h to exchange Na and Li ions. An ion exchange reaction with $LiNO_3$ (250 °C, 48 h) is also useful to obtain $LiCoO_2$ single crystals. After the reaction, the crystals were washed with distilled water repeatedly to remove Li_2CO_3 and Na_2CO_3. Chemical extraction of lithium from $LiCoO_2$ single crystals was carried out by immersing the crystals in an acetonitrile solution of NO_2BF_4 under argon atmosphere at 25–35 °C for 3 days. Molar ratio between $LiCoO_2$ and NO_2BF_4 was changed to control the Li content x ranging up to 1:2. The final products were washed with acetonitrile to remove $LiBF_4$. Synthesis of powder samples of Li_xCoO_2 by delithiation using NO_2BF_4 has been reported in the literature.[18] The Li content in the pristine and delithiated specimens was determined by inductively coupled plasma atomic emission spectroscopy (ICP-AES). In this study, we used Li_xCoO_2 single-crystal specimens with $x=0.99$ (pristine), 0.90, 0.71, 0.66, 0.46, and 0.25. To confirm the phase purity of the specimens, powder x-ray diffraction (XRD) was performed by a conventional diffractometer (RINT2200, Rigaku) using Cu $K\alpha$ radiation. Electrical resistivity was measured using a standard dc four-probe technique. dc magnetization measurements were carried out using superconducting quantum interference device magnetometer (MPMS, Quantum Design). Specific heat was measured by a thermal relaxation method on the physical property measurement system (PPMS, Quantum Design).

III. RESULTS AND DISCUSSION

A. Powder x-ray diffraction

In Fig. 1, powder XRD patterns for Li_xCoO_2 with $x=0.25-0.99$ are shown. Almost all of the peaks observed in XRD are indexed based on rhombohedral-type space group $R\bar{3}m$, indicating that the samples are of single phase, although a splitting of the peak into two is readily observed in (003), (006), and (009) reflections for the specimen with $x=0.90$. The peak split is due to the existence of two hexagonal phase region for $0.75 \leq x \leq 0.93$, which has been widely observed in the electrochemical oxidation process by earlier workers.[9,15,19–21] Figure 2 displays plots of lattice parameter c versus x together with the variation in c during the electrochemical Li deintercalation observed by *in situ* x-ray diffraction reproduced from Ref. 21. As seen in the figure, the variation in lattice parameter c of our specimens is consistent with that determined in the previous study. As the oxidation of Li_xCoO_2 proceeds, a monoclinic phase appears in the neighborhood of $x=0.5$ after the transition from hexagonal I to II for $0.75 \leq x \leq 0.93$, and hexagonal and monoclinic

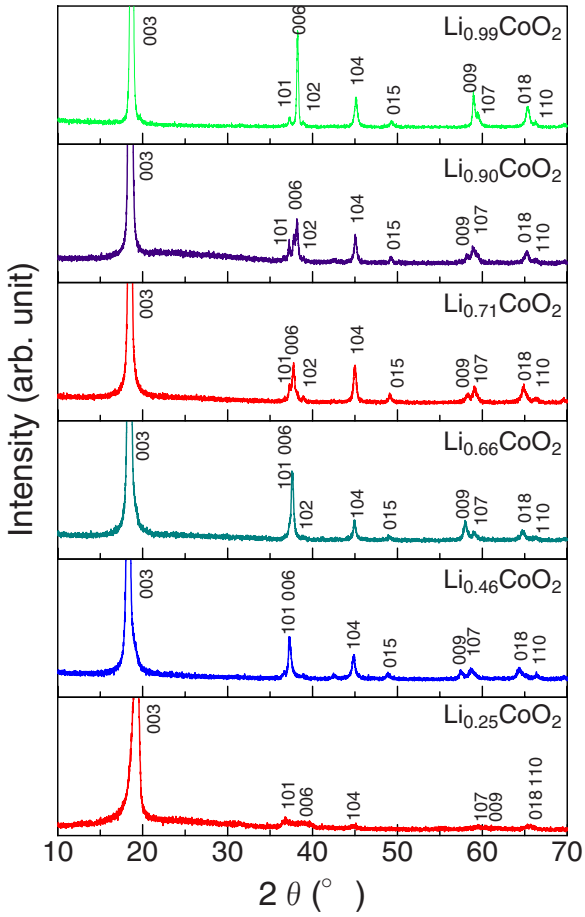

FIG. 1. (Color online) Powder x-ray diffraction patterns for Li_xCoO_2 with $x=0.25-0.99$.

phases coexist for $x \lesssim 0.20$.[19–21] We note that more detailed structural phase diagram including the region for $x<0.2$ has been recently proposed through the measurements of quasiopen-circuit voltage of Li_xCoO_2/Al cell.[15]

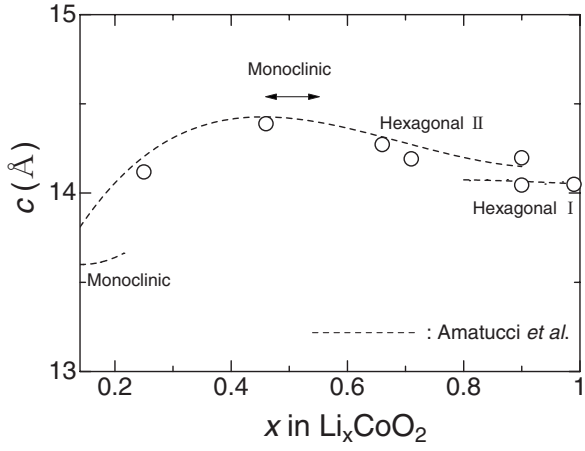

FIG. 2. Lattice parameter c for Li_xCoO_2 with $x=0.25-0.99$. The dotted lines show the variation in c for Li_xCoO_2 observed by *in situ* x-ray diffraction during the electrochemical Li deintercalation by Amatucci *et al.* (Ref. 21). Hexagonal and monoclinic phases appear in the oxidation process.

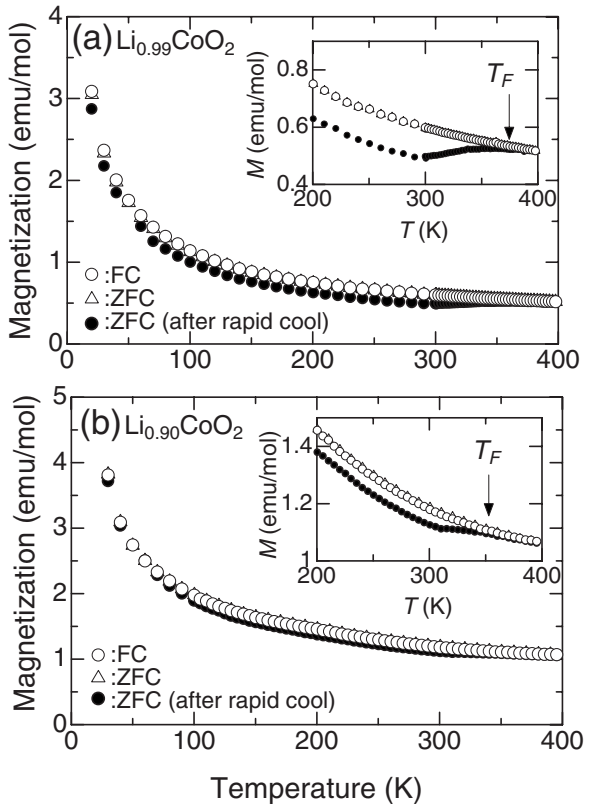

FIG. 3. Temperature dependence of dc magnetization measured with a magnetic field of $H=1$ T parallel to *ab* plane for Li_xCoO_2 with (a) $x=0.99$ and (b) 0.90. The measurements were done after rapid cool from above 400 to 10 K (closed circles) in addition to the measurements after slow cool down to 10 K (open symbols). The insets show closeups of the data for $200 \leq T \leq 400$ K.

B. dc magnetization

In Figs. 3(a) and 3(b), we show the results of the dc magnetization (M) measurements as a function of temperature (T) for Li_xCoO_2 with $x=0.99$ and 0.90 measured with an applied magnetic field of $H=1$ T parallel to *ab* plane under zero-field-cooled (ZFC) and field-cooled (FC) condition. In the measurements, dc magnetization was first measured up to 400 K after rapid cool of the sample from above 400 to 10 K in zero field. For rapid cool, the sample was once heated above 400 K in an electric furnace and quenched in acetonitrile at room temperature. This was followed by rapid sample insertion into the chamber of the magnetometer kept at 10 K. Then, the measurements were performed again after slow cool from 400 to 10 K at a rate −10 K/min in zero field and in a magnetic field of 1 T. As seen in Figs. 3(a) and 3(b), the $M(T)$ curve after slow cool both for $x=0.99$ and 0.90 appears to show a Curie-Weiss-type paramagnetic behavior and any difference is not observed in the FC and ZFC measurements, indicating the absence of magnetic order. On the other hand, the $M(T)$ curve after rapid cool for $x=0.99$ becomes different from those after slow cool below $T_F \sim 380$ K, as seen in the inset of Fig. 3(a). Also, it is found in the inset of Fig. 3(b) that the $M(T)$ curve for $x=0.90$ becomes thermal history dependent below $T_F \sim 350$ K.

In Figs. 4(a)–4(d), the $M(T)$ curves for Li_xCoO_2 with $x=0.25-0.71$ are shown. The measurements for $x=0.25-0.71$ were also performed both after rapid and slow cool in a similar manner to those for $x=0.90$ and 0.99. In Fig. 4(a), the $M(T)$ curves for $x=0.71$ exhibit a sharp decrease below $T_S \sim 155$ K. As shown in the inset of Fig. 3(a),

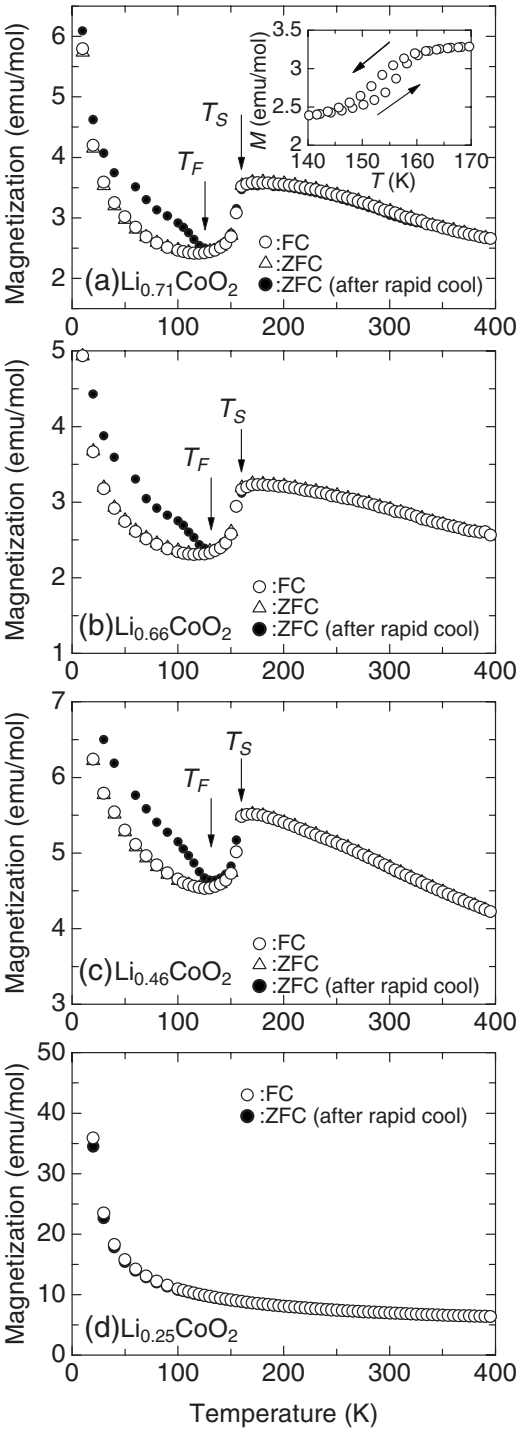

FIG. 4. Temperature dependence of dc magnetization measured with a magnetic field of $H=1$ T parallel to *ab* plane for Li_xCoO_2 with (a) $x=0.71$, (b) 0.66, (c) 0.46, and (d) 0.25. The measurements were done after rapid cool from 400 to 10 K (closed circles) in addition to the measurements after slow cool down to 10 K (open symbols). The inset shows the data collected during heating and cooling between 140 and 170 K for $x=0.66$.

TABLE I. Constant susceptibility χ_0, Weiss temperature Θ, Curie constant C, and effective magnetic moment μ_{eff} for Li_xCoO_2 with $x=0.99$, 0.90, and 0.25. These parameters were extracted from the $M(T)$ data ($10 \leq T \leq 400$ K) using Eq. (1).

x	χ_0 (emu/mol/Oe)	Θ (K)	C (emu/mol/K/Oe)	μ_{eff} (μ_B/Co)	μ_{eff} (μ_B/Co^{4+})
0.99	2.95×10^{-5}	−11	9.31×10^{-3}	0.273	2.73
0.90	7.33×10^{-5}	−9.4	1.40×10^{-2}	0.335	1.06
0.25	4.81×10^{-4}	−3.2	6.48×10^{-2}	0.720	0.831

a thermal hysteresis is observed in the $M(T)$ curve for $x=0.71$ around T_S, indicating the transition at T_S is of first order. These behaviors have been similarly observed in earlier studies.[10–15] Also it is found that there is no difference in the $M_{FC}(T)$ and $M_{ZFC}(T)$ curves after slow cool but the $M(T)$ curves after slow and rapid cool exhibit a splitting below $T_F \sim 130$ K. The characteristic behaviors of the $M(T)$ curve for $x=0.71$ are similarly observed for $x=0.66$ and 0.46 as seen in Figs. 4(b) and 4(c). It is noted that $T_S(\sim 155$ K) and T_F (~ 130 K) appears to be independent of Li content x for $0.46 \leq x \leq 0.71$. As shown later, T_F agrees with the temperature at which the motional narrowing in the ^{7}Li NMR linewidth is observed, indicating that the Li ions stop diffusing and stay at the regular site below T_F.

In Fig. 4(d), the $M(T)$ curve for $x=0.25$ is found to exhibit no anomaly contrasting to the sample with $0.46 \leq x \leq 0.71$ but a Curie-Weiss-type T dependence with no sign of magnetic order. $\chi(T)$ [$=M(T)/H$] curve for $x=0.99$, 0.90, and 0.25 observed in the FC measurements was fitted with the following formula:

$$\chi(T) = \chi_0 + \frac{C}{T-\Theta}, \tag{1}$$

where χ_0, C, and Θ denote the T-independent susceptibility, the Curie constant, and the Weiss temperature, respectively. Fitting parameters obtained from the fits of the $\chi(T)$ data ($10 \leq T \leq 400$ K) to Eq. (1) are summarized in Table I. In the table, effective magnetic moment μ_{eff} per Co atom was calculated from C, considering that all of the Co atoms are equivalent, while μ_{eff} per Co^{4+} was calculated assuming that all of the Co^{3+} ions are nonmagnetic ($S=0$). Although μ_{eff} per Co^{4+} is ~ 2.7 μ_B for $x=0.99$, μ_{eff} yields 1.73 μ_B corresponding to low spin Co^{4+} ($S=1/2$) if we assume $x \sim 0.975$. An error range $\Delta x = \pm 0.015$ of the composition determined by ICP may be possible for $x=0.99$. The value of μ_{eff} per Co^{4+} is reduced to ~ 1.1 μ_B for the sample with $x=0.90$, which is near the boundary between metallic and insulating states, as seen later. For $x=0.25$, μ_{eff} per Co^{4+} still has a large value of ~ 0.83 μ_B, whereas it has been reported that Li_xCoO_2 obtained by electrochemical oxidation is Pauli paramagnetic for $x \lesssim 0.35$.[15] In the table, it is found that Θ has a small negative value and χ_0 becomes larger with decreasing x probably due to the increase in Pauli paramagnetic component. These features are also found in the electrochemically delithiated specimens.[15]

C. Electrical resistivity

Next, we show the temperature dependence of electrical resistivity (ρ) for Li_xCoO_2 with $x=0.25-0.99$ in Figs. 5(a)–5(e). The data shown in the figures were collected during heating after slow cool down to ~ 10 K (~ -2 K/min). For $x=0.99$, the $\rho(T)$ curve exhibits an insulating behavior in Fig. 5(a). The $\rho(T)$ curve for $x=0.99$ was confirmed not to strictly obey an Arrhenius law, having a slightly temperature depending activation energy of $E_a \sim 0.03$ eV for $T=100-300$ K and ~ 0.02 eV for $T<100$ K. Also, an insulating behavior of $\rho(T)$ with an activation energy of 10^{-2} eV order which varies slightly with temperature has been ob-

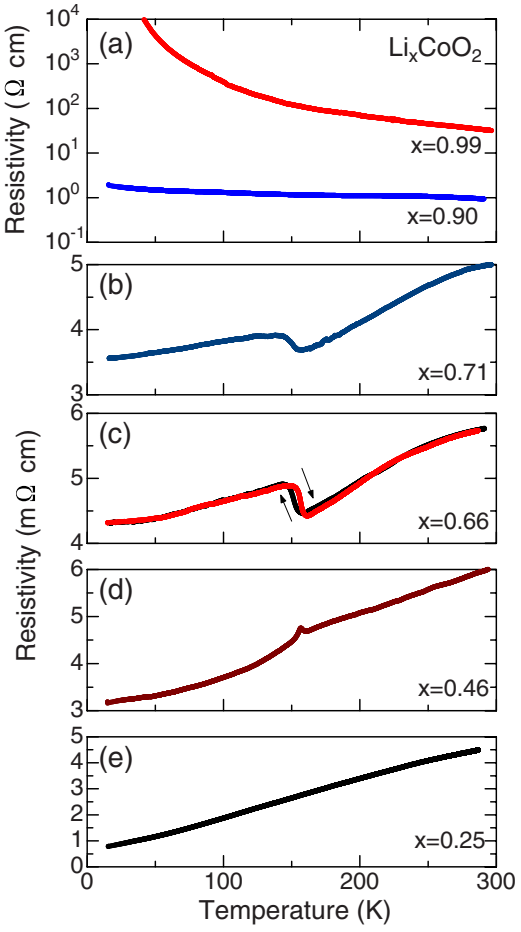

FIG. 5. (Color online) Temperature dependence of electrical resistivity measured along *ab* plane for Li_xCoO_2 with (a) $x=0.99$, 0.90, (b) 0.71, (c) 0.66, (d) 0.46, and (e) 0.25.

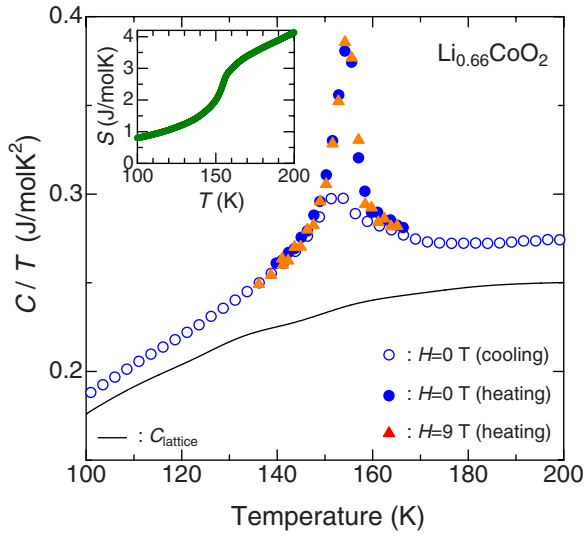

FIG. 6. (Color online) Plots of specific heat divided by temperature C/T versus temperature T for $Li_{0.66}CoO_2$ at $H=0$ and 9 T. The magnetic field was applied parallel to the c axis. The data were collected during heating (closed symbols) and cooling (open circles). The solid line represents the lattice contribution. The inset shows magnetic entropy versus temperature curve.

served in Li_xCoO_2 with $x=0.98-0.96$ in an earlier study.[9] For $x=0.90$, the $\rho(T)$ curve is nearly temperature independent with resistivity $\sim 10^0$ Ω cm, which is ~ 50 times smaller than that for $x=0.99$ at 300 K. In Fig. 5(b), the $\rho(T)$ curve for $x=0.71$ displays a metallic behavior with an amplitude of milliohm centimeter order. Thus, the critical Li content at which the system changes from an insulator to metal is likely to be near below 0.90. The $\rho(T)$ curve for $x=0.71$ shows a sudden increase below ~ 155 K, which corresponds to the first-order transition observed in the $M(T)$ curve at $T_S \sim 155$ K. Although a formation of charge-ordered state in CoO_2 layers has been expected for $x=2/3$,[15] no indicative of a transition into an insulating state is found in the $\rho(T)$ curve. However, we should note that the slope of the $\rho(T)$ curve for $x=0.71$ becomes smaller below the jump at $T_S \sim 155$ K, suggesting that the transport mechanism changes below T_S. The $\rho(T)$ curve for $x=0.66$ is qualitatively similar to that for $x=0.71$, as seen in Fig. 5(c). For $x=0.66$, the data collected during cooling are also shown. A slight thermal hysteresis is found in the jumplike anomaly at T_S as a result of the first-order character of the transition. The $\rho(T)$ curve for $x=0.46$ in Fig. 5(d) also shows an anomaly at $T_S \sim 155$ K but the anomaly is relatively small. In contrast, there is no anomaly in the $\rho(T)$ curve for $x=0.25$ in Fig. 5(e). Moreover, the residual resistivity of the $\rho(T)$ curve for $x=0.25$ is relatively small compared with that for higher x. The higher metallicity for $x=0.25$ may be associated with the absence of the transition at T_S.

D. Specific heat

Figure 6 displays plots of specific heat divided by temperature C/T versus T for $Li_{0.66}CoO_2$. The measurements were performed during cooling and heating after slow cool (-10 K/min). The data measured during heating show a sharp peak corresponding to the transition at $T_S \sim 155$ K while those measured on cooling show a small peak. A large thermal hysteresis is observed as a strong evidence of the first-order character of the transition at T_S. The measurements were also carried out in a magnetic field of $H=9$ T. The C/T peak at T_S is found to be not field dependent, indicating that the transition is not magnetic one. Assuming the occurrence of charge ordering at the fractional Li content $x=2/3$, the transition entropy is calculated as $\Delta S = -R(1/3 \ln 1/3 + 2/3 \ln 2/3) = 5.29$ J/mol K, which is the mixing entropy of Co^{3+}/Co^{4+} solution. To examine whether or not the transition entropy at T_S for $x=0.66$ corresponds to that of the charge ordering for $x=2/3$, we have estimated the entropy S as a function of T from the electronic contribution of specific heat C_e using the thermodynamic relationship,

$$S(T) = \int_0^T \frac{C_e}{T'} dT'. \tag{2}$$

C_e is given by subtracting the lattice contribution C_{lat} from the measured specific heat C. The $C_{lat}(T)$ data were estimated from the $C(T)$ data for insulating $Li_{0.99}CoO_2$. In the inset of Fig. 6, the $S(T)$ curve obtained by integrating C_e/T above 2 K is shown. The transition entropy is estimated to be $\Delta S \sim 1.9$ J/mol K for $T=140-170$ K. This value is 36% of the transition entropy of charge ordering for $x=2/3$, suggesting the possibility that the charge ordering is incomplete and a part of careers are localized. This scenario agrees with the result that $\rho(T)$ curve for $x=0.66$ exhibits a sudden increase at T_S but is still metallic below T_S. The transition entropy for Li_xCoO_2 with $x=0.67$ has been found to be $\Delta S = 1.49$ J/mol K from the magnitude of latent heat in the differential scanning calorimetry (DSC) measurements.[15] In a similar context, it has been argued from the smaller ΔS that the charge ordering is incomplete and a charge disproportionation, e.g., $2Co^{+3.5} \rightarrow Co^{+3.5+\delta} + Co^{+3.5-\delta}$ occurs.[15] Also for $x=0.71$, a sharp anomaly at T_S was observed in $C(T)/T$ data. For $x=0.46$, no distinct anomaly was however observed at T_S. This leads us to remember that the anomaly in the $\rho(T)$ curve for $x=0.46$ is relatively small compared to that for $x=0.66$ and 0.71. The DSC measurements have also revealed that the transition entropy for $x=0.50$ is $\Delta S=0.47$ J/mol K, which is considerably smaller than that for $x=0.67$.[15] Thus, it is inferred that the volume fraction of the charge ordering at T_S becomes continuously smaller with decreasing x and may be negligible for $x < 0.40-0.45$.

E. Plots of T_F versus Li content x

In the dc magnetic measurements, T_F, below which the $M(T)$ curve measured after rapid cool becomes different from that after slow cool, has been determined for each x. We show the plots of T_F versus x in Fig. 7, where T_S and the temperature at which the motional narrowing in the ^{7}Li NMR linewidth has been observed (T_{MN}) (Ref. 22) are plotted together. For higher $x(\geq 0.90)$, T_F decreases with decreasing x. In contrast, T_F is x independent for $x \lesssim 0.7$. It is found that the characteristic relationship between T_F and x are in good agreement with T_{MN} versus x data, suggesting that T_F

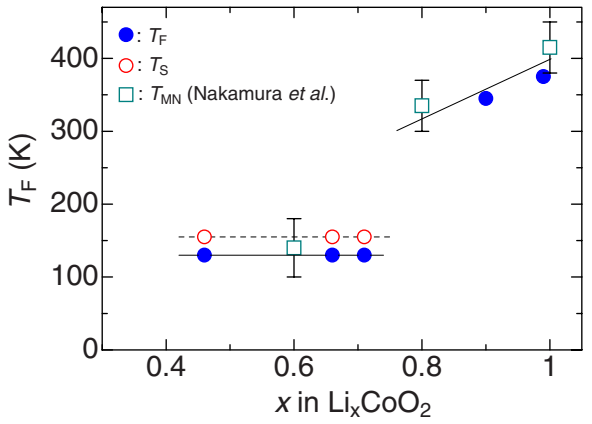

FIG. 7. (Color online) Plots of T_F versus x for Li_xCoO_2. T_S and T_{MN} are also plotted. T_{MN} is the temperature at which the motional narrowing in the ^{7}Li NMR linewidth has been observed (Ref. 22). The solid and dotted lines are guides for the eyes.

corresponds to the temperature above which Li ions start to diffuse from the regular site. This is also supported by the recent μ^+SR experiments on Li_xCoO_2, which have revealed that the Li diffusion starts above $T_d^{Li} \sim 150$ K both for $x=0.73$ and 0.53.[23] This fact is a firm evidence for the reliability of our result that the onset temperature of Li diffusion is x independent for $0.45 \lesssim x \lesssim 0.70$. The slight difference between T_d^{Li} (~ 150 K) and T_F (~ 130 K) may be due to the difference of the sample. The sample used in the μ^+SR experiments shows a sudden decrease in $M(T)$ at ~ 170 K, which is also slightly higher than $T_S \sim 155$ K of our specimens. We have found in this study that the difference in the $M(T)$ curve after slow and rapid cool is a reliable marker to detect the onset of Li diffusion.

F. Discussion

In Li_xCoO_2, Li ions stop diffusing and the ordering of Li ions is stabilized below T_F. The origin of the Li^+ ordering for $x \lesssim 0.7$ and $x \gtrsim 0.8$ is considered to be different from each other since T_F suddenly decreases and becomes constant for $x \lesssim 0.7$. As seen in Fig. 7, the first-order transition at T_S is always followed by the Li^+ ordering below $T_F \sim 130$ K, suggesting the possibility that the ordering of Li ions is triggered and stabilized by the charge ordering in CoO_2 layers below T_S, where electrons combine with cobalt ions. This situation reminds us an intimate correlation between Co^{3+}/Co^{4+} charge ordering and Na^+ ordering (zigzag chain) observed in $Na_{0.5}CoO_2$,[6] and also the characteristic ordering pattern of Na^+ vacancies in $Na_{0.75}CoO_2$ which provides an electrostatic landscape on the Co layers affecting the electronic and magnetic properties.[24–26] For $x=0.66$, we have observed a fairly small transition entropy at T_S compared with that expected in the transition into charge-ordered state for $x=2/3$, in addition to a metallic behavior in the $\rho(T)$ curve even below T_S. This suggests that the carrier localization below T_S is partial. Indeed, an electronic disproportionation at Co sites has been observed in $Na_{0.75}CoO_2$, where only 30% of the Co site form an ordered pattern of localized Co^{3+} states.[27] Moreover, we should note that this electronic texture in the CoO_2 layers would contribute to stabilizing the ordering of Na ions,[27] as recent calculation also suggest.[28] Thus, the charge ordering coupled with the Li^+ ordering in Li_xCoO_2 may be analogous to that observed in $Na_{0.75}CoO_2$. The difference in the aspects of charge ordering between Li_xCoO_2 and Na_xCoO_2 is however obvious since an insulating state is established by the complete charge ordering in $Na_{0.5}CoO_2$. To clarify the origin of the difference, the investigations on the ordering patterns of Li ions in Li_xCoO_2 at low T and comparison with that in Na_xCoO_2 are highly desirable.

Next, we focus on the behavior of $M(T)$ curve, which depends on thermal history showing a different amplitude of M for the measurements after rapid and slow cool, as shown in Figs. 3 and 4. The ordering pattern of Li ions after rapid cool is likely to be different from that after slow cool due to the glass-like freezing of the Li^+ motions by rapid cooling, and should be linked with the ordering of Co^{3+}/Co^{4+} via Coulomb interactions, which determines the amplitude of M. Thus, rapid cooling introduces disorder in Li layers, which would disturb the charge ordering in Co layers expected for $x=0.46-0.71$ below T_S. The destruction of the charge ordering may lead to the enhancement of M at low T since the $M(T)$ curve exhibits a sudden increase above T_S where the charge ordering is completely destroyed. In Figs. 4(a)–4(c), the amplitude of $M(T)$ after rapid cool is indeed enhanced compared to that after slow cool at low T and they coincide above T_F, where Li ions can diffuse so that the charge ordering in Co layers is reproduced. However, we could not observe a clear anomaly in the $\rho(T)$ curve at T_F for $x=0.46-0.71$ even in the measurement after rapid cool because the number of electrons which contributes to the metallic conductivity never changes across T_F. Forming a contrast, $M(T)$ measured after rapid cool is smaller than that after slow cool for $x=0.90$ and 0.99, as seen in Fig. 3. In this case, the arrangement of Li ions at high T also would be preserved by the freezing of Li^+ motions after rapid cool and the difference of $M(T)$ below T_F should also originate from the difference in the arrangements of Li ions below T_F. We note that the hysteresis observed for $x=0.99$ is rather larger than that for $x=0.90$. The larger hysteresis seems to be associated with the larger Li content in $Li_{0.99}CoO_2$, although the detailed mechanism is unclear. We could not rule out the possibility that Li layers are formed in an amorphous state by rapid cooling. If it is the case, the difference in the structure in Li layers could arise even for $x \sim 1.0$ and is necessary to explain the large thermal history dependence in the $M(T)$ curve for $x=0.99$.

IV. SUMMARY

In the present work, we have successfully obtained single crystals of Li_xCoO_2 with $x=0.25-0.99$ and performed the measurements of dc magnetization, electrical resistivity, and specific heat. It is found that the system changes from an insulator to metal at the critical Li content near below $x=0.90$ with decreasing x. A first-order phase transition is observed at $T_S \sim 155$ K for $x=0.46-0.71$. T_F below which the $M(T)$ curve becomes thermal history dependent is found to correspond to the onset temperature of Li^+ diffusion. For x

$=0.46-0.71$, the first-order transition at $T_S \sim 155$ K is always followed by the ordering of Li ions below $T_F \sim 130$ K, suggesting the possibility that the ordering of Li ions is triggered and stabilized by the charge ordering in Co layers. The transition entropy for $x=0.66$ estimated from the specific-heat anomaly is found to be 1.9 mJ/mol K, which is $\sim 36\%$ of that for the complete Co^{3+}/Co^{4+} charge ordering in $Li_{2/3}CoO_2$. In addition, the $\rho(T)$ curve for $x=0.66$ exhibits a sudden increase but still metallic below T_S. These facts suggest that the carrier localization below T_S is in part. It is inferred that the volume fraction of the charge ordering below T_S becomes continuously smaller with decreasing x and may be negligible for $x < 0.40-0.45$. For the further understanding, microscopic investigations on Li_xCoO_2 $(0.4 \leq x \leq 0.7)$ using single-crystal specimens are urgently required. Also, it is important to establish the ordering patterns of Li ions at low T since there would be a strong correlation between the ordering of Li^+ and the charge ordering in Co layers due to the electrostatic landscape provided by Li^+ ordering as in Na_xCoO_2.[24,26]

ACKNOWLEDGMENT

This work is financially supported by a Grant-in-Aid for Scientific Research (Grant No. 20540355) from the Japanese Ministry of Education, Culture, Sports, Science, and Technology.

[1] I. Terasaki, Y. Sasago, and K. Uchinokura, Phys. Rev. B **56**, R12685 (1997).
[2] K. Takada, H. Sakurai, E. Takayama-Muromachi, F. Izumi, R. A. Dilanian, and T. Sasaki, Nature (London) **422**, 53 (2003).
[3] M. L. Foo, Y. Wang, S. Watauchi, H. W. Zandbergen, T. He, R. J. Cava, and N. P. Ong, Phys. Rev. Lett. **92**, 247001 (2004).
[4] M. Yokoi, T. Moyoshi, Y. Kobayashi, M. Soda, Y. Yasui, M. Sato, and K. Kakurai, J. Phys. Soc. Jpn. **74**, 3046 (2005).
[5] G. Gašparović, R. A. Ott, J.-H. Cho, F. C. Chou, Y. Chu, J. W. Lynn, and Y. S. Lee, Phys. Rev. Lett. **96**, 046403 (2006).
[6] F. L. Ning, S. M. Golin, K. Ahilan, T. Imai, G. J. Shu, and F. C. Chou, Phys. Rev. Lett. **100**, 086405 (2008).
[7] K. Miyoshi, E. Morikuni, K. Fujiwara, J. Takeuchi, and T. Hamasaki, Phys. Rev. B **69**, 132412 (2004).
[8] T. Motohashi, R. Ueda, E. Naujalis, T. Tojo, I. Terasaki, T. Atake, M. Karppinen, and H. Yamauchi, Phys. Rev. B **67**, 064406 (2003).
[9] M. Ménétrier, I. Saadoune, S. Levasseur, and C. Delmas, J. Mater. Chem. **9**, 1135 (1999).
[10] D. G. Kellerman, V. R. Galakhov, A. S. Semenove, Ya. N. Blinvskov, and O. N. Leonidova, Phys. Solid State **48**, 548 (2006).
[11] J. Sugiyama, H. Nozaki, J. H. Brewer, E. J. Ansaldo, G. D. Morris, and C. Delmas, Phys. Rev. B **72**, 144424 (2005).
[12] K. Mukai, Y. Ikedo, H. Nozaki, J. Sugiyama, K. Nishiyama, D. Andreica, A. Amato, P. L. Russo, E. J. Ansaldo, J. H. Brewer, K. H. Chow, K. Ariyoshi, and T. Ohzuku, Phys. Rev. Lett. **99**, 087601 (2007).
[13] J. T. Hertz, Q. Huang, T. McQueen, T. Klimczuk, J. W. G. Bos, L. Viciu, and R. J. Cava, Phys. Rev. B **77**, 075119 (2008).
[14] K. Miyoshi, H. Kondo, M. Miura, C. Iwai, K. Fujiwara, and J. Takeuchi, J. Phys.: Conf. Ser. **150**, 042129 (2009).
[15] T. Motohashi, T. Ono, Y. Sugimoto, Y. Masubuchi, S. Kikkawa, R. Kanno, M. Karppinen, and H. Yamauchi, Phys. Rev. B **80**, 165114 (2009).
[16] S. Kawasaki, T. Motohashi, K. Shimada, T. Ono, R. Kanno, M. Karppinen, H. Yamauchi, and G.-q. Zheng, Phys. Rev. B **79**, 220514(R) (2009).
[17] F. C. Chou, J. H. Cho, P. A. Lee, E. T. Abel, K. Matan, and Y. S. Lee, Phys. Rev. Lett. **92**, 157004 (2004).
[18] S. Venkatraman and A. Manthiram, Chem. Mater. **14**, 3907 (2002).
[19] J. N. Reimers and J. R. Dahn, J. Electrochem. Soc. **139**, 2091 (1992).
[20] T. Ohzuku and A. Ueda, J. Electrochem. Soc. **141**, 2972 (1994).
[21] G. G. Amatucci, J. M. Tarascon, and L. C. Klein, J. Electrochem. Soc. **143**, 1114 (1996).
[22] K. Nakamura, H. Ohno, K. Okamura, Y. Michihiro, T. Moriga, I. Nakabayashi, and T. Kanashiro, Solid State Ionics **177**, 821 (2006).
[23] J. Sugiyama, K. Mukai, Y. Ikedo, H. Nozaki, M. Mansson, and I. Watanabe, Phys. Rev. Lett. **103**, 147601 (2009).
[24] M. Roger, D. J. P. Morris, D. A. Tennant, M. J. Gutmann, J. P. Goff, J.-U. Hoffmann, R. Feyerherm, E. Dudzik, D. Prabhakaran, A. T. Boothroyd, N. Shannon, B. Lake, and P. P. Deen, Nature (London) **445**, 631 (2007).
[25] F. C. Chou, M.-W. Chu, G. J. Shu, F.-T. Huang, W. W. Pai, H. S. Sheu, and P. A. Lee, Phys. Rev. Lett. **101**, 127404 (2008).
[26] D. J. P. Morris, M. Roger, M. J. Gutmann, J. P. Goff, D. A. Tennant, D. Prabhakaran, A. T. Boothroyd, E. Dudzik, R. Feyerherm, J.-U. Hoffmann, and K. Kiefer, Phys. Rev. B **79**, 100103(R) (2009).
[27] M.-H. Julien, C. de Vaulx, H. Mayaffre, C. Berthier, M. Horvatić, V. Simonet, J. Wooldridge, G. Balakrishnan, M. R. Lees, D. P. Chen, C. T. Lin, and P. Lejay, Phys. Rev. Lett. **100**, 096405 (2008).
[28] Y. S. Meng, A. Van der Ven, M. K. Y. Chan, and G. Ceder, Phys. Rev. B **72**, 172103 (2005).